Biochemistry

 Volume 33, Number 29 July 26, 1994

Accelerated Publications

Primary Charge Separation in Photosystem I: A Two-Step Electrogenic Charge Separation Connected with $P700^+A_0^-$ and $P700^+A_1^-$ Formation†

Birgit Hecks,‡ Karsten Wulf,‡ Jacques Breton,§ Winfried Leibl,§ and Hans-Wilhelm Trissl*,‡

Abteilung Biophysik, Fachbereich Biologie/Chemie, Universität Osnabrück, Barbarastrasse 11, D-49069 Osnabrück, Germany, and Section de Bioénergétique, Département de Biologie Cellulaire et Moléculaire, CEA-Saclay, F-91191 Gif-sur-Yvette Cedex, France

Received April 28, 1994; Revised Manuscript Received May 24, 1994®

ABSTRACT: A PS I membrane preparation from a PS II deficient mutant of *Synechocystis* sp. PCC 6803 (psb DI/DII/C⁻) was investigated by picosecond photovoltage and fluorescence measurements. The photovoltage kinetics show two distinct phases. At low excitation energies the fast phase correlates with the fluorescence decay time constant of 22 ± 4 ps. This phase is ascribed to the trapping of excitons as described by the reaction $(Ant_iP700)^* A_0 \rightarrow Ant_iP700^+ A_0^-$. In addition to this phase, the photovoltage displays a second rising phase of smaller amplitude with a time constant of 50 ± 15 ps. We assign the latter phase to further electron tranfer from A_0 to the secondary acceptor, A_1. Assuming the protein as a homogeneous dielectric, our results suggest that the transmembrane distance A_0–A_1 spans only a small part (20 ± 8%) of the distance P700–A_1.

Information on the structure of the reaction center and the electron carrier molecules involved in the primary photochemistry of photosystem I (PS I)[1] is less ample and less certain than in purple bacteria and even photosystem II (PS II). The crystallization of the reaction center of *Rhodopseudomonas viridis* and *Rhodobacter sphaeroides* and its high-resolution X-ray analysis have provided a precise knowledge of the positions of the electron carriers within the transmembrane protein (Deisenhofer et al., 1985; Deisenhofer & Michel, 1989; Feher et al., 1989; El-Kabbani et al., 1991). Although crystals of PS I from *Synechococcus* are available (Witt et al., 1988; Krauss et al., 1993), they presently allow only for a structure at low resolution. The assessment of intermediary electron carriers in PS I relies, therefore, on other, more indirect methods (Golbeck, 1987; Lagoutte & Mathis, 1989; Vos & van Gorkom, 1990; Ikeuchi, 1992).

Currently, the following electron carrier molecules and electron transfer steps in the PS I reaction center appear to be established [for recent reviews see Lagoutte and Mathis (1989), Golbeck and Bryant (1991), Golbeck (1992), Ikeuchi (1992), and Sétif (1992)]: The primary donor, P700, a dimer of chlorophyll molecules, reduces a primary acceptor, A_0, most likely a monomeric chlorophyll *a* molecule in the 10 ps time range. Different values for this time have been reported. The reaction seemingly depends on the antenna size and spectral composition of the particles used (Owens et al., 1987; Sétif, 1992). For low excitation densities it can be viewed as the trapping time as defined by the reaction:

$$(Ant_iP700)^*A_0 \xrightarrow{\tau_t} Ant_iP700^+A_0^-$$

Subsequently, the electron is transferred to a secondary acceptor, A_1, a phylloquinone (Brettel et al., 1986; Itoh et al., 1987; Snyder et al., 1991), and in following steps to iron–sulfur centers, F_X, F_A, and F_B, which become reduced with multiphasic kinetics in the time range from 15 to 200 ns

† This work was financially supported by the Deutsche Forschungsgemeinschaft (Sonderforschungsbereich 171, TP-A1).

* To whom correspondence should be addressed.
‡ Universität Osnabrück.
§ CEA Saclay.

® Abstract published in *Advance ACS Abstracts,* June 15, 1994.

[1] Abbreviations: A_0, primary acceptor (chlorophyll *a* monomer); A_1, secondary acceptor (phylloquinone); F_X, F_A, F_B, iron–sulfur centers; MV, methylviologen; P700, primary donor of PS I; PMS, phenazine methosulfate; PS I (II), photosytem I (II); PSU, photosynthetic unit; RC, reaction center.

0006-2960/94/0433-8619$04.50/0

(Brettel, 1988; Mathis & Sétif, 1988; Sétif & Brettel, 1993; Lüneberg et al., 1994). The electron transfer from A_0 to A_1 has been reported to occur in times shorter than 50 ps (Nuijs et al., 1986; Shuvalov et al., 1986; Holzwarth et al., 1993; Hastings et al., 1994b).

In reaction centers of purple bacteria and PS II the primary transmembrane charge separation (<1 ns) proceeds in essentially two electrogenic steps (Deprez et al., 1986; Trissl & Leibl, 1989). Two fast electrogenic steps may also be discernible in the case of PS I. These are the formation of the radical pair states, $P700^+ A_0^-$, and $P700^+ A_1^-$. Further, presumably electrogenic reactions, occur on a slower time scale (Brettel, 1988; Sétif & Brettel, 1993). From electroluminescence measurements it has been concluded that P700 A_0 spans 30%, A_0 A_1 50%, and A_1 F_A 20% of the membrane (Vos & van Gorkom, 1990). Although at least the latter value is at variance with the picture that emerges from X-ray crystallography (Krauss et al., 1993), the proposed significant electrogenicity assigned to A_0 A_1 electron transfer should allow direct detection of this reaction by photoelectric methods. Until now photovoltage measurements could not contribute to the assessment of these relative distances since the time resolution (Trissl et al., 1987) or the signal-to-noise ratio (Trissl et al., 1993b) was not sufficient to resolve two electrogenic steps when both are faster than 100 ps.

In this contribution we applied a fast photovoltage technique with improved time resolution and improved data analysis to resolve the electron transfer from $P700^*$ to A_0 and A_1 within the core of the reaction center of PS I. To avoid any interference with electrogenic reactions from PS II, we used membranes isolated from a mutant of *Synechocystis* sp. PCC 6803 that lacks essential subunits of the PS II core. The applied technique probes both the kinetics of exciton and electron transfer reactions as well as the relative dielectrically weighted transmembrane distances between the electron carriers. In addition, we applied time-resolved fluorescence decay measurements to confine the numerical values of rate constants for trapping and for quenching by reaction centers with oxidized donor, $P700^+$.

MATERIALS AND METHODS

The cell culture (*Synechocystis* sp. PCC 6803 psb DI/DII/C$^-$) was a gift from Dr. W. Vermaas. This mutant is devoid of the D1 and D2 subunits of PS II as well as CP43 (Vermaas et al., 1990). The cells were grown in liquid media of BG 11 supplemented with 5 mM glucose, 30 μg/mL chloramphenicol, 25 μg/mL spectinomycin, and 25 μM atrazine at 25 °C. The light intensity was adjusted to about 50 $\mu E\ m^{-2}\ s^{-1}$. The cells were harvested in the late logarithmic growth phase. PS I particles were prepared as described elsewhere (Bottin & Sétif, 1991).

The Chl *a*/P700 ratio was determined from the maximal absorption change of $P700^+$ at 700 and 820 nm, using the differential molar absorption coefficients of 64 and 6.5 $mM^{-1}\ cm^{-1}$, respectively (Hiyama & Ke, 1972; Mathis & Sétif, 1981). This yielded a Chl *a* antenna size of $N = 75 \pm 15$. To estimate the presence of long-wavelength absorbing chlorophylls, a low temperature (77 K) fluorescence spectrum was recorded. The main peak was at 722 nm. The spectrum was very similar to that of a corresponding PS I preparation from the wild type.

For photovoltage measurements the membranes suspended in 2 mM MES (pH 6.0) were irreversibly oriented in the capacitor microcoaxial cell previously described (Trissl et al., 1987) by applying a DC voltage of 10 V for 100 ms. After this orientation procedure, the membranes sedimented onto the platinum plate were overlayed with 10 mM ascorbate and 50 μM PMS. The photovoltage signals were stable for at least 1 h.

The excitation source was either a frequency doubled Nd-YAG laser (FWHM = 30 ps) used for fluorescence measurements or a dye laser (FWHM = 8 ps; maximal energy ca. 500 μJ) used for photovoltage measurements. After passing an optical delay of 15 m the beam was focused by a collimating lens to a diameter of approximately 4 mm.

Details of the setups for photovoltage and fluorescence measurements are described in Trissl and Wulf (1994) and data analysis in Wulf and Trissl (1994). In order to yield maximal time resolution, the photovoltage was not amplified but directly recorded as single shots on a transient digitizing oscilloscope (model 7450, Tektronix). Typically, 40 single-shot traces were averaged before data analysis. Fluorescence was measured from the front surface of a flat (0.1 mm) cuvette and detected at wavelengths in the range between 665 and 730 nm (K 70 filter; Balzers) by a Si-Avalanche photodiode (BPW 28, Telefunken). The signals were amplified 40-fold by a broad band GHz amplifier (model SHF-75S; SHF-Design; 100 kHz–7 GHz).

The primary photophysical and photochemical reactions were described by a set of differential equations (Wulf & Trissl, 1994) similar to the ones published before (Leibl et al., 1989; Trissl et al., 1993a). The analysis program takes into account the accelerated speed of formation of the primary radical pair at higher excitation energies and the nonlinear effects caused by excitation energy annihilation as well as the finite duration of the laser flash. Similarly, the apparatus response, $g(t)$, is approximated by a Gauss function of the width σ according to

$$g(t) = \frac{g_0}{\sqrt{2\pi}\sigma} e^{-(t/\sqrt{2}\sigma)^2}$$

The analysis was restricted to two electrogenic phases with an electrogenicity ratio, e_2. The time constants for loss processes of the excited state other than by trapping, quenching by $P700^+$, and exciton–exciton annihilation were fixed to τ_1 = 2.5 ns (Gulotty et al., 1985).

RESULTS

A typical photoelectric response from oriented PS I membranes upon excitation with a 8-ps laser flash is shown in Figure 1a (dots). The rising phase is significantly slower than the rise time of the apparatus that was determined by calibration measurements with oriented purple membranes (Figure 1a, dashed line). The decaying phase, due to the discharge of the measuring cell into the 50 Ω input impedance of the amplifier, was determined by analysis of photovoltage traces from PS I membranes recorded on slower time bases (not shown). These two apparative characteristics were taken into account in the data analysis program (Wulf & Trissl, 1994).

The slower rise of the PS I photovoltage cannot satisfactorily be fitted with a single exponential phase with a time constant of 22 ps (i.e., trapping time, see below) as shown by the residual plot in Figure 1c. Much better fits were obtained when a second electrogenic phase with a time constant, τ_2, was allowed as shown in Figure 1a (solid line) and in Figure 1b by the corresponding residuals. We attribute the first phase to the primary step of charge separation (trapping) and the second to a further electron transfer step. As the kinetics of both phases are not well separated, the determination of unique

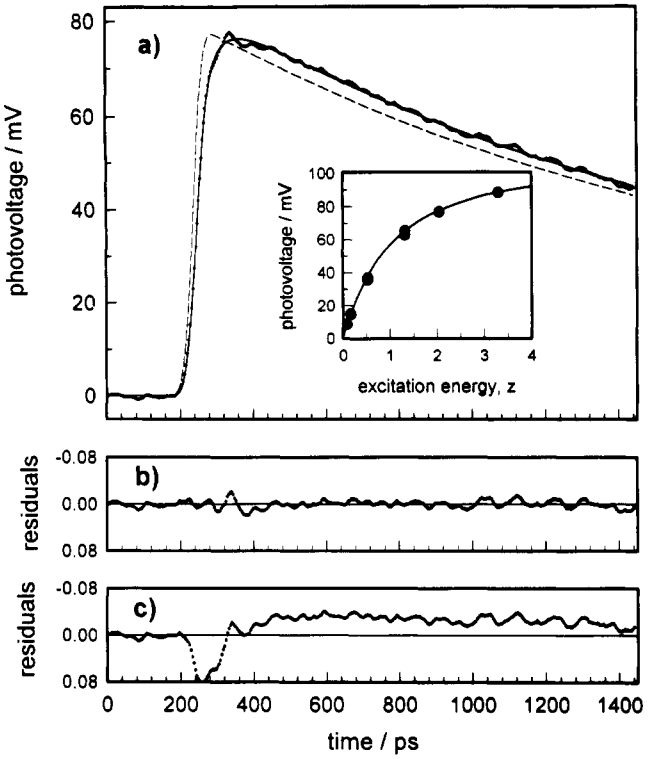

FIGURE 1: Photovoltage of irreversibly oriented PS I membranes excited with 8-ps flashes at 677 nm. (a) Original data and calculated trace with the following parameters obtained from the best fit: excitation energy z = 2.0; annihilation time constant, 15 ps; time constant of quenching of $P700^+$, 22 ps; trapping time constant, 22 ps; time constant of second step of charge separation, 46 ps; relative electrogenicity of second step, 0.27. (b) Residuals for best fit. (c) Residuals for the case that only one electrogenic reaction occurs with the trapping time constant. (Inset of panel a) Dependence of the peak photovoltage on the relative laser flash energy (saturation curve). Parameters for calculation of the theoretical curve: trapping time constant, 22 ps; time constant for quenching of $P700^+$, 22 ps; second step of charge separation, 50 ps; relative electrogenicity of second step, 0.25;. annihilation time constant, 15 ps.

values for time constants and electrogenicity factors is difficult. Furthermore, two other rate constants that influence the kinetics of the signal should also be considered. These are the rate constant of quenching by $P700^+$, k_c, and the annihilation rate constant, γ. In the following we will describe how the numerical values of these parameters are determined by independent experiments and appropriate data analysis.

At very low excitation energy, the first phase represents the trapping time which is defined as the time constant for primary charge separation in the low energy limit. At higher excitation energy, when more than one exciton per photosynthetic unit (PSU) is created ($z > 1$), the trapping kinetics are affected by two processes; first, the trapping kinetics speed up due to the bimolecular interaction between excitons and RCs, and, second, the excitons may get lost by annihilation. Then the first phase of the photovoltage rise becomes nonexponential and dependent on three main parameters: (i) the trapping time constant, τ_t, (low energy limit), (ii) the annihilation time constant, and (iii) the excitation energy. All three can partially compensate each other in fit routines. However, in a final fit the first two parameters are invariable with respect to the excitation energy.

The trapping time was determined by two different methods, photovoltage and time-resolved fluorescence measurements. In the low energy limit, the trapping kinetics become independent of the excitation energy and the annihilation is negligible. When the photovoltage traces obtained at very

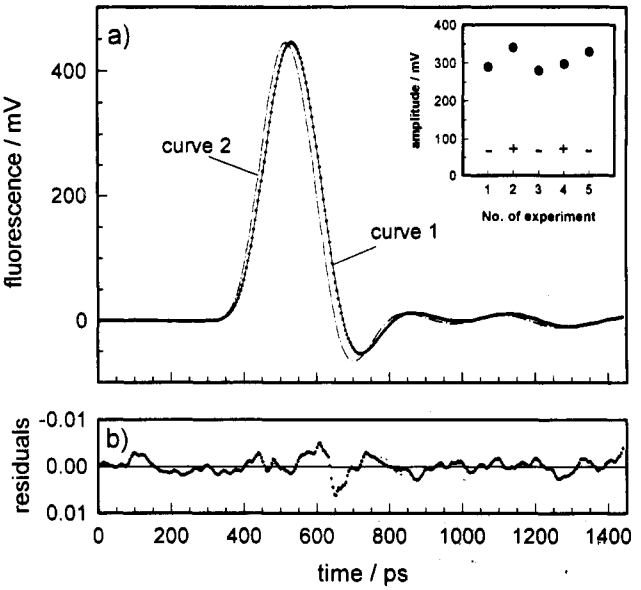

FIGURE 2: Fluorescence decay kinetics of nonoriented PS I membranes (5 mM ascorbate, 10 μM PMS, and 50 μM MV) in a 100-μm flat measuring cuvette excited with 30-ps flashes at 532 nm in the low energy limit ($z \approx 0.05$). (a) Data (curve 1, dots) and best fit (curve 1, line) resulting from a convolution of a 23-ps exponential phase with the fluorescence response from purple membranes (curve 2). Note the shift of the two curves which originates from the very fast fluorescence decay of the purple membranes (<1 ps) compared to the slower trapping time of the PS I membranes (about 22 ps). (b) Residuals of best fit. (Inset in panel a) Fluorescence amplitudes of the same sample with the primary donor P700 in the reduced (no background light, –) or oxidized state (background light, +).

low excitation energies were subjected to three parameter fits (τ_t, τ_2, and e_2), a trapping time, τ_t = 20 ± 10 ps, was found. In order to determine the trapping time with higher precision than allowed by the photovoltage measurements, time-resolved fluorescence measurements were also performed. These experiments were done in the low-energy limit of excitation where the fluorescence decay is solely due to trapping. The fluorescence transient from nonoriented PS I membranes is shown in Figure 2a (curve 1). It is slower than the response time of the detection system which was obtained with purple membranes (Figure 2a, curve 2). Purple membranes display a fluorescence decay kinetics of 0.5 ps (Dobler et al., 1988; Song et al., 1993). This response was therefore taken as a calibration standard for the time resolution of the fluorescence apparatus, and this trace was used for convolution with exponential functions. The time constant that gave the best fit to the fluorescence from PS I membranes was τ_t = 22 ± 4 ps. A component with a long lifetime (2.5 ns) and a very small relative amplitude (about 10^{-3}) was assigned to "unconnected" chlorophylls. The fluorescence kinetics of this preparation were also measured with the single photon timing method yielding the same result (Gatzen and Holzwarth, unpublished results).

The fluorescence yield and the fluorescence decay kinetics were also measured in samples with oxidized primary donor in order to estimate the quenching property of $P700^+$. Complete oxidation was ensured by adding either the electron acceptor methylviologen (MV) or ferricyanide and applying strong background illumination in both cases. The results were independent of the acceptor used. The fluorescence transients give the same time constants as for the open state (data not shown). In addition, there was no difference in fluorescence amplitudes within an experimental error of ±10% when the redox state of P700 was reversibly changed between the reduced and oxidized state by switching the background

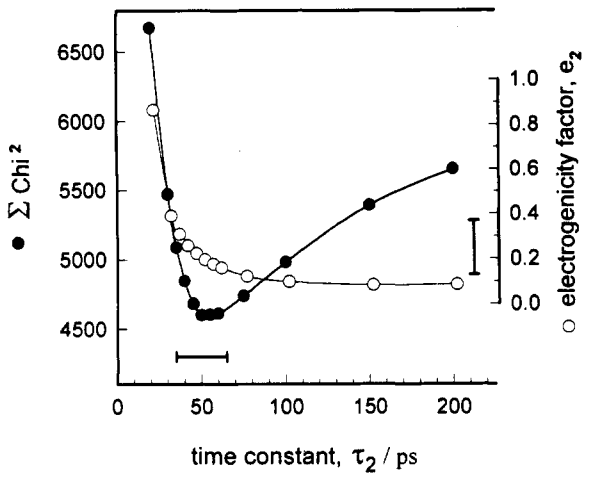

FIGURE 3: Dependence of $\sum_{i=1}^{11}\chi_i^2$ on the time constant, τ_2. The right-hand scale indicates the relative electrogenicity, e_2, belonging to these time constants as determined by the best fit to all traces (Figure 1, inset). The magnitude of the first step of charge separation is set to 1. The error bars for the time constant, τ_2 (bottom), and the relative electrogenicity, e_2 (right), are indicated.

light on and off in the presence of MV as artificial electron acceptor (Figure 2a, inset). Hence, the quenching rate constant of $P700^+$ equals the trapping rate constant, $k_c = k_t$.

Increasing the excitation energy leads to an acceleration of the first phase of the photovoltage (trapping kinetics) as well as to larger amplitudes. In Figure 1a (inset, dots) is shown the peak photovoltage versus the excitation energy that was varied by neutral density filters (saturation curve). The vertical and horizontal scales for the data points were adjusted to give the best fit to a theoretical saturation curve calculated with the parameters listed in the legend. This procedure is based on the following rationale: the vertical scale is freely adjustable since it depends on experimental parameters, such as the degree of orientation of the membranes or the amount of membranes present in the cell. In contrast, the horizontal scale of the theoretical curve is calibrated in the dimensionless quantity z (absorbed photons per PSU). Thus, the adjustment of the experimental curve yields the correlation of the relative excitation energy with the normalized scale, z. (It turned out that this procedure is much more precise than measuring the absolute excitation energy of the focused laser beam at the position of the microcoaxial cell.)

The saturation curve in Figure 1a (inset) can also be used to confine the rate constant for exciton–exciton annihilation, γ, since the curvature strongly depends on this parameter. Hence, such fits allow the determination of the annihilation rate constant. We found that for the PS I membranes used the rate constant for losses by annihilation is approximately 2 times larger than the rate constant for trapping. Hence, for PS I the parameter, α, that describes the competition between annihilation and trapping as introduced by Deprez et al. (1990) is $\alpha \approx 1$.

To quantify the relative amplitude of the second step of charge separation with the highest possible precision, all photovoltage data were analyzed simultaneously. The essence of this data analysis was to extract a common set of fit parameters for all kinetic traces belonging to a saturation curve by minimizing the sum of χ^2 (this is based on the fact that within a saturation curve all fit parameters must be invariable). The remaining parameters are the time constant, τ_2, and the electrogenicity factor, e_2. In Figure 3 are plotted the sum of the χ^2 from 11 traces at different energies vs the time constant of the second electrogenic step, τ_2. The right-hand scale gives the electrogenicity factor, e_2, corresponding to a given τ_2. The other parameters involved have been determined as described before. From Figure 3 it can be concluded that our data are best fitted by a two-step primary charge separation in the subnanosecond time domain: the first step (electrogenicity factor, $e_1 = 1$) reflects trapping and the second step reflects charge stabilization with $\tau_2 = 50 \pm 15$ ps and an electrogenicity factor of $e_2 = 0.25 \pm 0.13$.

DISCUSSION

The present experiments were carried out with flat PS I membranes prepared from a PS II-deficient mutant psb DI/DII/C⁻ of the cyanobacterium *Synechocystis* sp. PCC 6803 (Vermaas et al., 1990). The preparation was shown to possess approximately 75 Chl *a* molecules per P700. The spectral composition of the antenna pigments of the mutant membranes is very similar to that of membranes from the wild type as shown by the close similarity of the 77 K fluorescence spectra (data not shown).

By analysis of the fluorescence decay kinetics and photovoltage rise kinetics, we find a trapping time of 22 ± 4 ps, which is compatible with trapping times reported for similar preparations (Wasielewski et al., 1987; Holzwarth et al., 1993; Hastings et al., 1994a). Our results demonstrate that fast photovoltage and fluorescence measurements yield consistent trapping times and thus complement each other in this respect. However, both methods provide different information concerning the further electron transfer.

As trapping in PS I is known to be essentially irreversible, there is no way to detect further electron transfer steps within the reaction center by fluorescence. In contrast, photovoltage techniques offer an attractive way to follow secondary electron transfer steps via intermediary acceptors within the reaction center. These secondary steps manifest themselves by additional rising phases in the photovoltage (Deprez et al., 1986; Trissl & Leibl, 1989). Their analysis is straightforward if the kinetic phases due to trapping (formation of the primary radical pair) and secondary electron transfer are sufficiently separated in time. This, however, is not the case in PS I. Here the trapping time of about 22 ps interferes strongly with the electron transfer from A_0 to A_1. To separate both phases, we made use of the fact that the trapping kinetics can be accelerated by increasing the excitation energy (i.e., exciton concentration) whereas the rate constant of electron tansfer from A_0 to A_1 is independent of the excitation energy. The acceleration of trapping kinetics is due to the bimolecular reaction between excitons and RCs. For a δ-function excitation that is 5-fold oversaturating, we calculate actual trapping kinetics of less than 5 ps. This is the basis for being able to resolve electrogenic phases that (at low energy) occur with a time constant similar to that of trapping.

The time resolution of the photovoltage and fluorescence setup as defined by the broadening of a δ-function input to a Gauss function output was $\sigma = 20$ ps and $\sigma = 35$ ps, respectively. However, as shown by control experiments with purple membranes, the deconvolution of signals with high signal-to-noise ratio allows the analysis of exponential time constants down to 15 ps in photovoltage and 5 ps in fluorescence measurements (Trissl & Wulf, 1994). In addition, the global fit procedure applied in this work is essential in confining the numerical values.

For the forward electron transfer in PS I we find a reoxidation kinetics of A_0 of ≈50 ps. This value is compatible with several other reports on a corresponding electron transfer step (Nuijs et al., 1986; Shuvalov et al., 1986). In a recent

picosecond transient absorption study by Holzwarth et al. (1993) the A_0^- state could not be traced within their accessible time window of >40 ps. The authors concluded that either A_0 is not a Chl *a* at all, or electron transfer occurs directly from $P700^*$ to A_1, or that reoxidation of A_0 occurs in <40 ps. Our photovoltage data clearly argue against the latter two possibilities. The data rather establish an intermediary acceptor (A_0) located between P700 and A_1. Its transient concentration on the picosecond time scale can be shown by computer simulations to depend on the trapping time of the particles used and also on the excitation energy applied. This may be the reason for this state not having been detected in the above mentioned study. High transient concentrations of A_0^- may be reached when preparations with fast trapping times are used (small antenna size) and/or when the excitation energy is increased, as was the case in the present study.

In a recent picosecond absorption spectroscopy study, Hastings et al. (1994b) investigated the same mutant as in the present work and also used high excitation energy. They analyzed their absorption transients due to $A_0^- \rightarrow A_0$ by a 21-ps time constant but gave no error estimation. Forcing this value into our data leads to systematic poor fits and drifts in the residual plots. Hence, this time constant is incompatible with our data. The faster time constant of 21 ps found by Hastings et al. could be due to the stronger annihilation present in their experiments ($z \approx 4$–8) compared to ours ($0.2 \leq z \leq 3$) and to the neglect of this nonlinear effect in their analysis. Measurements of small absorption changes in the region where antenna chlorophylls absorb are much more susceptible to small variations in parameters than the photovoltage measurements especially in the regime of strong exciton annihilation. Under oversaturating conditions the absorption changes increase with exciton density whereas photovoltage signals saturate. In addition, a small difference in quenching between P700 and $P700^+$ would affect much more the analysis of differential absorption change measurements than the analysis of photovoltage kinetics.

The present photovoltage data demonstrate a two-step primary charge separation in PS I occurring in less than 100 ps. A first phase, intimately related to the exciton dynamics, is attributable to the conversion of the excited state into the radical pair $P700^+ A_0^-$. The process is conveniently termed "trapping", and its kinetics in the low energy limit are described by the "trapping time". A second electrogenic step occurs with a time constant of 50 ± 15 ps. It is attributed to further electron transfer to a secondary acceptor, probably A_1. Assuming a homogeneous dielectric within the RC, the electron transfer between A_0 and A_1 spans much less transmembrane distance than the one between P700 and A_0 (Figure 4, middle).

Our result is incompatible with the results of Vos and van Gorkom (1990) by electroluminescence measurements which yielded just the reverse distance relationship between these redox components (Figure 4, left). This discrepancy might be due to the very indirect measuring method in which many parameters are involved that are difficult to assess experimentally. In particular, it was assumed by Vos and van Gorkom that the $P700^+ F_A^-$ charge pair distance corresponds to the membrane thickness. However, F_A and F_B are located on a polypeptide protruding out of the membrane, and therefore they might be exposed to a local dielectric constant which is significantly higher than that inside the lipid membrane layer. Beside this, the interpretation of the electroluminescence measurements relied on the assumption that all reactions occur after vibrational relaxation. This condition might not be fulfilled for the primary charge separation on the time scale of a few picoseconds (Vos et al., 1993).

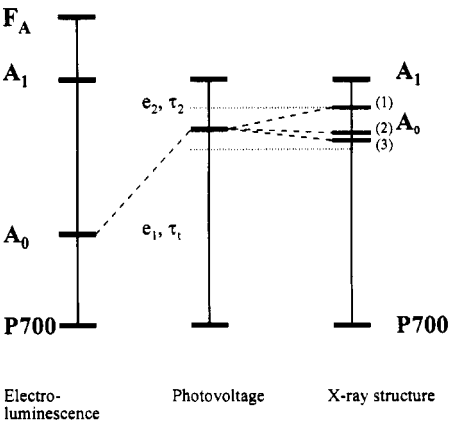

FIGURE 4: Proposed transmembrane locations of redox components in PS I according to different methods. The horizontal bars indicate the approximate center-to-center distances normalized to the distance P700 A_1. (Left) Electroluminescence (Vos & van Gorkom, 1990); (middle) present work; (right) X-ray structure (Krauss et al., 1993). The dashed lines connect the estimated locations of A_0, and the dotted lines indicate the error in the photovoltage measurements. The different positions of A_0 (right) represent the three alternative positions of A_1 indicated in (Krauss et al., 1993). These positions were estimated by projection of the center of the phylloquinone onto the axis formed by the center of the chlorophyll dimer and F_x taking into account the respective normalizations to P700 A_1. Position 1 applies to the location favored by Krauss et al., whereas positions 2 and 3 refer to the nearly symmetrical locations [white dots in Figure 2c of Krauss et al. (1993)].

The ratio of the distances between P700 and A_0 and between A_0 and A_1 determined in this work can be compared with the structural information emerging from X-ray analysis of PS I core crystals (Krauss et al., 1993). This structural model suggests only 13% electrogenicity for the second phase if the first phase is normalized to 100% (Figure 4, right, position 1). However, alternative locations for phylloquinone molecules were also indicated which correspond to a somewhat larger electrogenicity of about 30% (Figure 4, right, positions 2 and 3). Although the error bars in the photovoltage measurements do not allow a clear distinction between these different locations, our data favor the largest distance between A_0 and A_1. Further support for this model comes from the observation that the electrogenicities of the A_1 F_x and A_0 A_1 electron transfer steps are comparable (W. Leibl, unpublished results). The position of F_x being well resolved in the X-ray structure, the transmembrane location of A_1 should thus be about midway between A_0 and F_x.

Our result agrees with the assignment of A_0 being located relatively far from P700 (Krauss et al., 1993). Notably, A_0 is not one of the two chlorophyll monomers found near P700. These monomers could be the equivalent of the corresponding ones in the bacterial reaction center and may be involved in the very first step of charge separation (Moser et al., 1991; Arlt et al., 1993). The location of A_1 with respect to A_0 favored by Krauss et al. results in an asymmetric arrangement of the cofactors. As pointed out previously (Golbeck, 1993; Nitschke & Rutherford, 1994), this seems hardly compatible with the fact that two quinone molecules as well as two symmetrical A_0 acceptors are present in PS I and that the homology between the two large subunits forming the PS I RC is even higher than in purple bacteria where a symmetric arrangement of the cofactors is found. The alternative proposal of Krauss et al. (1993), which is more compatible with our photovoltage data than their favored one, indicates two rather symmetric positions for the phylloquinone molecules. Thus, the PS I reaction center reveals similarities to the RC of purple bacteria

suggesting that the latter can serve as a model even for PS I. This also strengthens the idea of a common structural principle and of an evolutionary relationship of all photosynthetic RCs (Nitschke & Rutherford, 1991). If the RC of purple bacteria is taken as a reference, PS I may be viewed as a much faster version and the RC of heliobacteria (Nuijs et al., 1985a) and green sulfur bacteria (Nuijs et al., 1985b) as a slower version with respect to the charge stabilization reaction.

ACKNOWLEDGMENT

We thank Dr. W. Vermaas for the mutant strain of *Synechocystis* sp. PCC 6803 (psb DI/DII/C$^-$) and Dominique Dejonghe for technical assistance. We also thank Prof. Dr. W. Junge for general support and laboratory facilities.

REFERENCES

Arlt, T., Schmidt, S., Kaiser, W., Lauterwasser, C., Meyer, M., Scheer, H., & Zinth, W. (1993) *Proc. Natl. Acad. Sci. U.S.A. 90*, 11757–11761.

Bottin, H., & Sétif, P. (1991) *Biochim. Biophys. Acta 1057*, 331–336.

Brettel, K. (1988) *FEBS Lett. 239*, 93–98.

Brettel, K., Sétif, P., & Mathis, P. (1986) *FEBS Lett. 203*, 220–224.

Deisenhofer, J., & Michel, H. (1989) *EMBO J. 8*, 2149–2170.

Deisenhofer, J., Epp, O., Miki, K., Huber, R., & Michel, H. (1985) *Nature 318*, 618–624.

Deprez, J., Trissl, H.-W., & Breton, J. (1986) *Proc. Natl. Acad. Sci. U.S.A. 83*, 1699–1703.

Deprez, J., Paillotin, G., Dobek, A., Leibl, W., Trissl, H.-W., & Breton, J. (1990) *Biochim. Biophys. Acta 1015*, 295–303.

Dobler, J., Zinth, W., Kaiser, W., & Oesterhelt, D. (1988) *Chem. Phys. Lett. 144*, 215–220.

El-Kabbani, O., Chang, C. H., Tiede, D., Norris, J. R., & Schiffer, M. (1991) *Biochemistry 30*, 5361–5369.

Feher, G., Allen, J. P., Okamura, M. Y., & Rees, D. C. (1989) *Nature 339*, 111–116.

Golbeck, J. H. (1987) *Biochim. Biophys. Acta 895*, 167–204.

Golbeck, J. H. (1992) *Annu. Rev. Plant Physiol. Plant Mol. Biol. 43*, 293–324.

Golbeck, J. H. (1993) *Curr. Opin. Struct. Biol. 3*, 508–514.

Golbeck, J. H., & Bryant, D. A (1991) in *Current Topics in Bioenergetics* (Lee, C. P., Ed.) Vol. 16, pp 83–177, Academic Press, Inc., San Diego and New York.

Gulotty, R. J., Mets, L. J., Alberte, R. S., & Fleming, G. R. (1985) *Photochem. Photobiol. 41*, 487–496.

Hastings, G., Kleinherenbrink, F. A. M., Lin, S., & Blankenship, R. E. (1994a) *Biochemistry 33*, 3185–3192.

Hastings, G., Kleinherenbrink, F. A. M., Lin, S., McHugh, T. J., & Blankenship, R. E. (1994b) *Biochemistry 33*, 3193–3200.

Hiyama, T., & Ke, B. (1972) *Biochim. Biophys. Acta 267*, 160–171.

Holzwarth, A. R., Schatz, G., Brock, H., & Bittersmann, E. (1993) *Biophys. J. 64*, 1813–1826.

Ikeuchi, M. (1992) *Plant Cell Physiol. 33*, 669–676.

Itoh, S., Iwaki, M., & Ikegami, I. (1987) *Biochim. Biophys. Acta 893*, 508–516.

Krauss, N., Hinrichs, W., Witt, I., Fromme, P., Pritzkow, W., Dauter, Z., Betzel, C., Wilson, K. S., Witt, H. T., & Saenger, W. (1993) *Nature 361*, 326–331.

Lagoutte, B., & Mathis, P. (1989) *Photochem. Photobiol. 49*, 833–844.

Leibl, W., Breton, J., Deprez, J., & Trissl, H.-W. (1989) *Photosynth. Res. 22*, 257–275.

Lüneberg, J., Fromme, P., Jekow, P., & Schlodder, E. (1994) *FEBS Lett. 338*, 197–202.

Mathis, P., & Sétif, P. (1981) *Isr. J. Chem. 21*, 316–320.

Mathis, P., & Sétif, P. (1988) *FEBS Lett. 237*, 65–68.

Moser, C. C., Keske, J. M., Warncke, K., & Dutton, P. L. (1991) *Biophys. J. 59*, 521a.

Nitschke, W., & Rutherford, A. W. (1991) *Trends Biochem. Sci. 16*, 241–245.

Nitschke, W., & Rutherford, A. W (1994) in *Origin and Evolution of Biological Energy Conservation* (Baltscheffsky, M., Ed.) VCH Publishers, New York.

Nuijs, A. M., van Dorssen, R. J., Duysens, L. N. M., & Amesz, J. (1985a) *Proc. Natl. Acad. Sci. U.S.A.. 82*, 6865–6868.

Nuijs, A. M., Vasmel, H., Joppe, H. L. P., Duysens, L. N. M., & Amesz, J. (1985b) *Biochim. Biophys. Acta 807*, 24–34.

Nuijs, A. M., Shuvalov, V. A., van Gorkom, H. J., Plijter, J. J., & Duysens, L. N. M. (1986) *Biochim. Biophys. Acta 850*, 310–318.

Owens, T. G., Webb, S. P., Mets, L. J., Alberte, R. S., & Fleming, G. R. (1987) *Proc. Natl. Acad. Sci. U.S.A. 84*, 1532–1536.

Sétif, P. (1992) in *The Photosystems: Structure, Function and Molecular Biology* (Barber, J., Ed.) pp 471–499, Elsevier Science Publishers, Amsterdam and London.

Sétif, P., & Brettel, K. (1993) *Biochemistry 32*, 7846–7854.

Shuvalov, V. A., Nuijs, A. M., van Gorkom, H. J., Smit, H. W. J., & Duysens, L. N. M. (1986) *Biochim. Biophys. Acta 850*, 319–323.

Snyder, S. W., Rustandi, R. R., Biggins, J., Norris, J. R., & Thurnauer, M. C. (1991) *Proc. Natl. Acad. Sci. U.S.A. 88*, 9895–9896.

Song, L., El-Sayed, M. A., & Lanyi, J. K. (1993) *Science 261*, 891–894.

Trissl, H.-W., & Leibl, W. (1989) *FEBS Lett. 244*, 85–88.

Trissl, H.-W., & Wulf, K. (1994) *Biophys. J.* (submitted).

Trissl, H.-W., Leibl, W., Deprez, J., Dobek, A., & Breton, J. (1987) *Biochim. Biophys. Acta 893*, 320–332.

Trissl, H.-W., Gao, Y., & Wulf, K. (1993a) *Biophys. J. 64*, 984–998.

Trissl, H.-W., Hecks, B., & Wulf, K. (1993b) *Photochem. Photobiol. 57*, 552–568.

Vermaas, W. F. J., Charité, J., & Eggers, B. (1990) in *Current Research in Photosynthesis* (Baltscheffsky, M., Ed.) Vol. I, pp 231–238, Kluwer Academic Publishers., Dordrecht, The Netherlands.

Vos, M. H., & van Gorkom, H. J. (1990) *Biophys. J. 58*, 1547–1555.

Vos, M. H., Rappaport, F., Lambry, J.-C., Breton, J., & Martin, J.-L. (1993) *Nature 363*, 320–325.

Wasielewski, M. R., Fenton, J. M., & Govindjee (1987) *Photosynth. Res. 12*, 181–190.

Witt, I., Witt, H. T., Di Fiore, D., Rögner, M., Hinrichs, W., Saenger, W., Granzin, J., Betzel, C., & Dauter, Z. (1988) *Ber. Bunsen-Ges. Phys. Chem. 92*, 1503–1506.

Wulf, K., & Trissl, H.-W. (1994) *Biophys. J.* (submitted).